Electron Transport in Ru and Os Polybenzimidazole-Based Metallopolymers†

Colin G. Cameron,‡ Timothy J. Pittman, and Peter G. Pickup*

Department of Chemistry, Memorial University of Newfoundland, St. John's, Newfoundland, Canada A1B 3X7

Received: March 12, 2001; In Final Form: June 27, 2001

A series of conjugated polymer−redox polymer hybrids based on the complexation of poly-(bibenzimidazoles) with bis-(2,2′-bipyridyl)Ru^{2+} and bis-(2,2′-bipyridyl)Os^{2+} has been prepared to investigate the effects of electronic communication between metal centers through the conjugated backbone. Electron transport rates in the mixed valence M(III/II) states have been measured as electron diffusion coefficients (D_e) by impedance spectroscopy and dual (sandwich) electrode voltammetry. D_e values are generally higher than for nonconjugated Ru(2,2′-bipyridyl)$_3^{3+/2+}$-type polymers, and their dependencies on the metal (Os or Ru), pH and nature of the polymer backbone are consistent with significant contributions from superexchange mechanisms. Hole-type superexchange appears to dominate in the Ru polymers, while a number of observations indicate that electron-type superexchange may dominate for the Os complexes.

Introduction

Polymeric materials in which metals are coordinated directly to a long-range π network have attracted significant attention in recent years.[1,2] They offer much promise in the development of nanoelectronics, electrocatalysts, sensors, and optical devices. Perhaps more importantly they are leading to the discovery of new chemical and electronic processes. For example, Yamamoto and co-workers[3] have reported that complexes of $RuCl_3$ with polypyridine and polybipyridine exhibit notable photocatalytic cleavage of water to H_2. Wolf and Wrighton[4] have demonstrated that the electron density at a rhenium coordinated to a conjugated polymer, poly[5,5′-(2-thienyl)-2,2′-bithiazole], can be modulated by the electron density of the polymer. Swager and co-workers have developed a series of polymetallorotaxanes for sensory[5] and molecular electronic applications.[6] Most recently, they have reported an architecture in which a central conjugated strand is isolated by two metal containing strands.[7]

One anticipated advantage of an arrangement in which the metal is coordinated to the π backbone lies in the premise that an interaction between the metal-based dπ orbitals and the polymer π or π^* orbitals will occur. This can provide additional mechanisms for electron transport between metal centers and facilitate the movement of electrons necessary for high electrocatalyst performances or rapid switching in devices.

Electron transport in redox polymers has been shown to occur by at least three mechanisms, as illustrated schematically in Figure 1. In saturated systems, outer-sphere electron exchange between redox sites (outer-sphere mechanism) provides the only significant contribution to electron transport. In unsaturated systems, and particularly in highly conjugated systems, electron transport can also occur through the polymer backbone by mediated and/or superexchange mechanisms. These are distinguished by the availability of redox states of suitable energy on the polymer to mediate electron transport. If such states are available, the electron can hop between a localized metal-based redox site, a polymer-based site, and a second metal site in two steps (mediated mechanism). If such states are not available, then electron transfer through the backbone must result from a mixing of appropriate orbitals of both metals with the HOMO and/or LUMO of the backbone (superexchange). Previously, we have demonstrated the existence of superexchange mechanisms in several benzimidazole-based metallopolymers,[8−10] and several new examples are presented here. This paper also explores further the factors that determine the rate of superexchange electron transport and attempts to elucidate pathways.

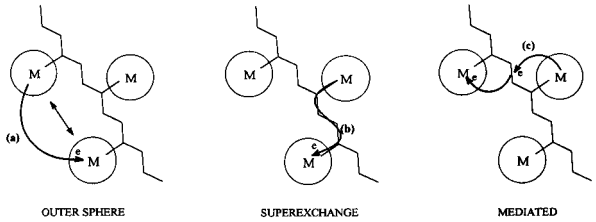

Figure 1. Mechanisms for electron transfer between metal sites in a metallopolymer.

It will be assumed that the well-known bimetallic superexchange mechanisms[11] are applicable to the extended systems considered here. The essence of metal−ligand−metal interactions in a mixed valence conjugated bridging complex is shown schematically in Figure 2.[12] Two formal pathways are possible: (1) hole-type superexchange, where the ligand donates an electron from its HOMO to fill a dπ vacancy in the metal in the higher oxidation state (the hole thus formed is filled by an electron from the other metal), and (2) electron-type superexchange, where an electron from the lower valence metal is promoted to the ligand π^* orbital and subsequently falls into the other metal's dπ orbitals. The dominant pathway will depend on the relative energy levels of the metal dπ orbitals and the bridging ligand's π or π^* orbitals, and the ease with which this exchange may occur depends on the absolute energy gap between the metal and ligand orbitals for the preferred pathway.

To probe the effects of the metal redox potential and polymer backbone structure on the electron transport kinetics and mechanism, we have investigated the complexes of three different polymer backbones with both $Os(bpy)_2^{2+}$ and $Ru(bpy)_2^{2+}$ (bpy = 2,2′-bipyridine). The three polymer backbones

† Part of the special issue "Royce W. Murray Festschrift".

* To whom correspondence should be addressed (Email: ppickup@mun.ca)

‡ Current Address: Beckman Institute, mail code 139-74, Caltech, Pasadena, CA 91125.

10.1021/jp0109325 CCC: $20.00
Published on Web 08/16/2001

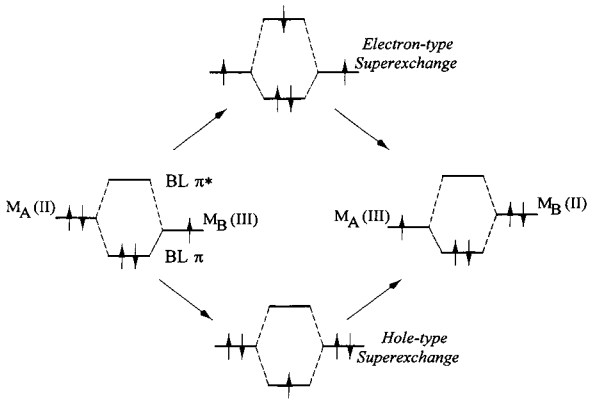

Figure 2. Proposed models for electron exchange through a π-conjugated bridging ligand (BL). (Adapted from ref 12.)

employed in this work (structures **1** to **3**) differ in the bibenzimidazole portion, which is either a bibenzimidazole ($(PhIm)_2$) or a benzobisimidazole (Im_2Ph), and the linkage between these units, which is either a pyridine (Py) or a pyrazine (Pz) ring. Hence, they are abbreviated as poly(Py-$(PhIm)_2$), poly(Py-Im_2Ph), and poly(Pz-$(PhIm)_2$).

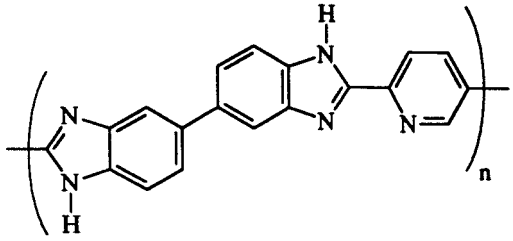

1

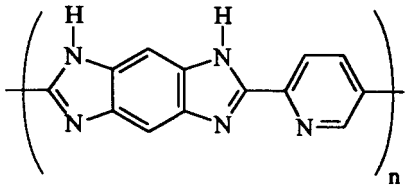

2

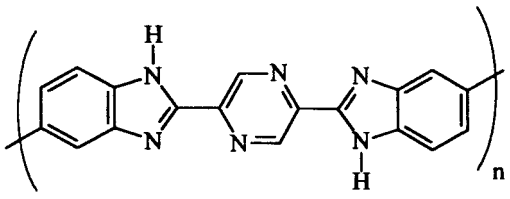

3

Experimental Section

Materials. Polyphosphoric acid was generated as required by stirring a 1:1.8 mass ratio mixture of H_3PO_4 (85%) and P_2O_5 under nitrogen at 100 °C for 24 h, and then cooling to room temperature. 2,5-Pyrazinedicarboxylic acid was prepared from 5-methyl-2-pyrazinecarboxylic acid (Aldrich) by oxidation with $KMnO_4$ in NaOH(aq), precipitated with HCl(aq), and recrystallized from water as a pale orange solid in 36% yield. Ru(bpy)$_2$Cl$_2$ and Os(bpy)$_2$Cl$_2$ were prepared according to literature methods.[13] Acetonitrile was distilled over calcium hydride. Tetraethylammonium perchlorate was prepared according to a literature method[14] and triply recrystallized from water. Tetraminobenzene tetrahydrochloride (Aldrich) was recrystallized from HCl(aq) as described by Jenekhe.[15] 3,3′-Diaminobenzidine (Aldrich, 99%) was recrystallized twice from H_2O. 2,5-Pyridinedicarboxylic acid (Aldrich, 98%), phosphorus pentoxide (Fisher), 85% phosphoric acid (Anachemia), and all other chemicals were used as received.

Instrumentation. Unless stated otherwise, all potentials are reported against a SSCE reference electrode. Electrochemical experiments were performed using a Pine Instruments RDE4 bipotentiostat, a Solartron (Schlumberger) 1268 electrochemical interface and 1250 frequency response analyzer, or a EG&G PAR 273A potentiostat and 5210 lock-in amplifier.

Synthesis. *Poly[(6,6′-bibenzimidazole-2,2′-diyl)-2,5-pyridine] (poly(Py-(PhIm)$_2$), **1**).* The synthesis and characterization of this polymer has been previously reported.[9]

*Poly[(1,7-dihydrobenzo{1,2-d:4,5-d′}-bisimidazole-2,6-diyl)-2,5-pyridine] (poly(Py-Im$_2$Ph), **2**).* Polyphosphoric acid (30 g) was prepared and thoroughly degassed by repeated evacuations and flushes with N_2. Recrystallized tetraminobenzene tetrahydrochloride (0.690 g, 2.43 mmol) was added at r.t., and the flask was slowly warmed to 100 °C in a N_2 stream. HCl gas removal was completed by repeated cycles of evacuations and N_2 flushes. 2,5-Pyridinedicarboxylic acid (0.414 g, 2.48 mmol) was added, and the reaction mixture was stirred under N_2 at 100 °C for 48 h. The temperature was then raised to 120 °C and P_2O_5 (1.4 g, 10 mmol) was added. The reaction was stirred for 48 h at 120 °C, and finally for 24 h at 143 °C.

The resulting polymer was precipitated from the cooled reaction mixture by stirring it into H_2O (900 mL). Following 24 h of stirring, the orange solid was collected by filtration and then suspended in 0.2 M NaOH(aq) (900 mL), stirred for 3 days, and collected again by filtration. Finally it was suspended in H_2O (900 mL) for 48 h, collected by filtration and dried in vacuo to give a dark gray solid with a metallic luster (0.562 g, 74%). Elemental analysis: Calculated for $C_{13}H_7N_5 \cdot 4.5H_2O$: C 49.68%, H 5.10%, N 22.29%. Found C 50.51%, H 4.21%, N 21.78%. FTIR (KBr, cm^{-1}): 3388 (br), 3172 (br), 1641 (m), 1597 (s), 1454 (vs), 1385 (s), 1352 (s), 1284 (s), 1240 (m,br), 1052 (m), 843.

*Poly[(6,6′-bibenzimidazole-2,2′-diyl)-2,5-pyrazine] (poly(Pz-(PhIm)$_2$), **3**).* 3,3′-Diaminobenzidine (1.65 g, 7.7 mmol) and 2,5-pyrazinedicarboxylic acid (1.30 g, 7.7 mmol) were added together to polyphosphoric acid (27 g) at r.t. The reaction was stirred under N_2 at 95 °C for 24 h, and at 112 °C for 60 h. P_2O_5 (4.0 g, 28 mmol) was then added and the reaction was allowed to proceed for a further 16 h at 150 °C.

The dark red solution was cooled to r.t. and stirred into water (1 L), giving a red solid that was collected by filtration. The solid was washed by stirring for 24 h in each of three batches of water (1 L). Drying under vacuum gave 2.6 g (76%) of product as a dark green brittle solid. Elemental analysis: Calculated for $C_{18}H_{10}N_6 \cdot 7.25H_2O$: C 49.03%, H 5.60%, N 19.06%. Found C 49.08%, H 4.19%, N 19.03%. FTIR (KBr, cm^{-1}): 3417 (br), 1628 (vs), 1578 (m), 1518 (s), 1443 (s), 1312 (s), 1170 (s), 897 (m,br), 806 (s).

Bisbipyridylruthenium(II) complex of poly Poly[(6,6′-bibenzimidazole-2,2′-diyl)-2,5-pyridine] (poly{[Ru{Py-(PhIm)$_2$}-(bpy)$_2$](ClO$_4$)$_2$}). The synthesis of this metallopolymer has been previously described.[9]

Bisbipyridylruthenium(II) complex of Poly[(1,7-dihydrobenzo-{1,2-d:4,5-d′}-bisimidazole-2,6-diyl)-2,5-pyridine] (poly{[Ru-(Py-Im$_2$Ph)(bpy)$_2$](ClO$_4$)$_2$}). **Caution! Perchlorates are potentially dangerous.** While no detonation tendencies have been observed for these compounds, standard precautions should be taken.

$Ru(bpy)_2Cl_2 \cdot 2H_2O$ (0.0899 g, 0.173 mmol) and poly(Py-Im_2Ph) (0.0390 g, 0.127 mmol·site) were refluxed for 4 days in glycerol (50 mL) under N_2. Dilution with two volumes of water, filtration, and addition of a large excess of saturated aqueous $NaClO_4$ solution to the filtrate produced a red solid, which was collected by filtration and then stirred in water (20 mL) overnight. The solid was again collected by filtration, washed with water then diethyl ether, and then air-dried to give 0.124 g (100% yield) of a fine red-brown solid. Elemental analysis: Calculated for $C_{33}H_{23}N_9O_8Cl_2Ru \cdot H_2O \cdot C_3H_8O_3$: C 45.24%, H 3.48%, N 13.19%. Found: C 45.16%, H 3.12%, N 13.23%.

Bisbipyridylruthenium(II) complex of poly[(6,6′-bibenzimidazole-2,2′-diyl)-2,5-pyrazine] (poly{[Ru{Pz-(ImPh)$_2$}(bpy)$_2$]-(ClO_4)$_2$}). $Ru(bpy)_2Cl_2 \cdot 2H_2O$ (0.0980 g, 0.188 mmol) and poly(Pz-$(PhIm)_2$) (0.0308 g, 0.070 mmol·site) were refluxed in glycerol (50 mL) for 3 days. The resulting red liquid was cooled to r.t., filtered (leaving no residue), diluted with H_2O (200 mL), and filtered again. Addition of a large excess of saturated aqueous $NaClO_4$ solution precipitated a green solid which was collected by filtration, rinsed copiously with water and air-dried to give 0.130 g (108%) of a dark green solid. Elemental analysis: Calculated for $C_{18}H_{10}N_6(C_{20}H_{16}N_4Cl_2O_8Ru)_{1.95} \cdot (H_2O)(C_3H_8O_3)_2$: C 44.34%, H 3.50%, N 11.33%. Found C 44.51%, H 3.18%, N 11.24%.

A similar polymer complex with lower Ru content was prepared analogously, with only one equivalent of $Ru(bpy)_2Cl_2 \cdot 2H_2O$ having been used.

Bisbipyridylosmium(II) complex of poly[(6,6′-bibenzimidazole-2,2′-diyl)-2,5-pyridine] (poly{[Os{Py-(PhIm)$_2$}(bpy)$_2$]-(ClO_4)$_2$}). $Os(bpy)_2Cl_2$ (0.118 g, 0.207 mmol) and poly(Py-$(PhIm)_2$) (0.061 g, 0.157 mmol·site) were refluxed together in glycerol (50 mL) for 6 days. The resulting dark solution was filtered and diluted with H_2O (300 mL). A large excess of solid $NaClO_4$ was added, and the resulting red precipitate was collected by filtration. It was then stirred in a large volume of water overnight and collected by filtration again, giving 0.148 g (90%) of a fine black powder. Elemental analysis: Calculated for $C_{19}H_{11}N_5(C_{20}H_{16}N_4Cl_2O_8Os) \cdot 2H_2O$: C 44.75%, H 2.98%, N 12.04%, Cl 6.77%. Found C 45.26%, H 3.21%, N 11.01%, Cl 6.16%.

Bisbipyridylosmium(II) complex of Poly([6,6′-bibenzimidazole-2,2′-diyl]-2,5-pyrazine) (poly{[Os{Pz-(ImPh)$_2$}(bpy)$_2$]-(ClO_4)$_2$}). $Os(bpy)_2Cl_2$ (0.045 g, 0.079 mmol) and poly(Pz-$(PhIm)_2$) (0.011 g, 0.025 mmol·site) were refluxed in glycerol (25 mL) under N_2 for 4 days. Dilution of the resulting dark solution with two volumes of water, filtering, and addition of excess solid $NaClO_4$ to the filtrate produced a dark green-brown solid, which was collected and then stirred in H_2O (20 mL) overnight. The resulting black solid was collected by filtration, rinsed with water then ether, and air-dried to give 39.8 mg (80%) of a fine black solid. Elemental analysis: Calculated for $C_{18}H_{10}N_6(C_{20}H_{16}N_4Cl_2O_8Os)_{1.95} \cdot 3.4C_3H_8O_3$: C 40.53%, H 3.46%, N 9.71%. Found C 40.95%, H 3.12%, N 9.31%.

Purity of the Metallopolymers. The absence of monomeric Ru complexes in the poly{[Ru{Py-$(PhIm)_2$}$(bpy)_2$]$(ClO_4)_2$} sample was established by gel permeation chromatography.[9] For the other metallopolymers, the absence of significant extraction of colored species into CH_2Cl_2 and the absence of electrochemical waves characteristic of $M(bpy)_2X_2$ and $M(bpy)_3$ species were taken as sufficient evidence that monomeric complexes had been removed during washing.

Film Preparation. Films of the metallopolymers were cast onto Pt or glassy carbon disk electrodes from solutions in *N,N*-dimethyl acetamide, DMF, or water saturated nitromethane.

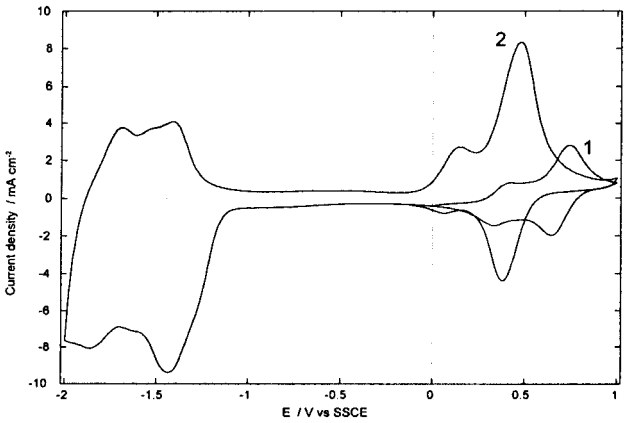

Figure 3. Cyclic voltammetry (100 mV s^{-1}) of poly[Os{Py-$(PhIm)_2$}-$(bpy)_2$] on a Pt disk electrode in CH_3CN containing 0.1 M Et_4NClO_4. Scan numbers are indicated.

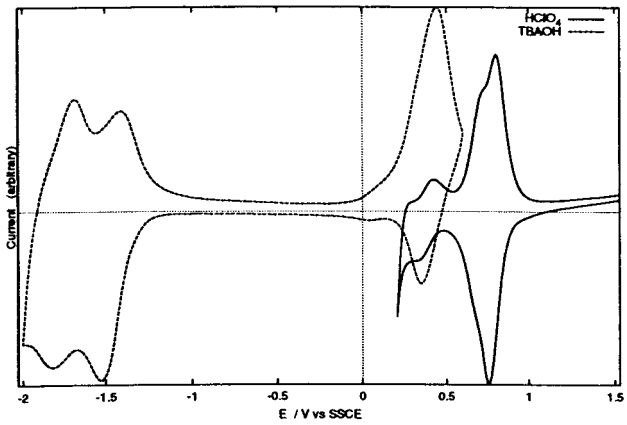

Figure 4. Cyclic voltammetry (100 mV s^{-1}) of poly[Os{Py-$(PhIm)_2$}-$(bpy)_2$] on a Pt disk electrode in CH_3CN containing 0.1 M Et_4NClO_4 and $HClO_4$ or Bu_4NOH.

Results and Discussion

Cyclic Voltammetry. The cyclic voltammetry of poly[Ru{Py-$(PhIm)_2$}$(bpy)_2$] has been described in detail elsewhere.[9] A redox wave due to the Ru(III/II) couple appears in the range of ca. 0.8 V to 1.2 V vs SSCE, depending on the degree of protonation of the polymer backbone, and a pair of bipyridine-based reductions appear at −1.47 and −1.77 V vs SSCE (in neutral CH_3CN). The Ru(III/II) half-wave potential changes by −63 mV pH^{-1} in the pH 2−4 range, consistent with a one-proton, one-electron process, and a pK_a of ca. 5. The voltammetric behavior of poly[Ru{Py-Im_2Ph}$(bpy)_2$] is similar to that of poly[Ru{Py-$(PhIm)_2$}$(bpy)_2$] and so will not be discussed.

Figures 3 and 4 show voltammograms of films of poly[Os{Py-$(PhIm)_2$}$(bpy)_2$] on Pt electrodes in neutral, acid, and basic CH_3CN. The first scan in the neutral electrolyte (Figure 3) shows Os(III/II) waves at ca. +0.4 V and +0.8 V and several ligand-based reduction waves in the −1 to −2 V region. Cycling through these reduction waves causes (a) the appearance of a new Os(III/II) wave at ca. +0.15 V, (b) a large increase in the size of the +0.4 V wave, and (c) disappearance of the +0.8 V wave. As previously discussed for the Ru analogue,[9] these changes arise from an increase in pH resulting from the reduction of water in the film or electrolyte. As shown by the voltammograms recorded under acidic and basic conditions (Figure 4), the +0.8 V formal potential corresponds to the protonated polymer, while that at +0.4 V corresponds to the deprotonated form. However, this explains neither the presence of the small wave at +0.15 V in the neutral electrolyte (second

TABLE 1: Formal Potentials (V vs SSCE) of the Metallopolymers

	M(III/II)			
complex	acid	base	bpy1(0/−1)	bpy2(0/−1)
poly[Ru{Py-$(PhIm)_2$}$(bpy)_2$]	1.24	0.79	−1.47	−1.77
poly[Ru{Py-Im_2Ph}$(bpy)_2$]	1.23			
poly[Ru{Pz-$(PhIm)_2$}$(bpy)_2$]	1.13, 1.29	*a*	*b*	*b*
poly[Os{Py-$(PhIm)_2$}$(bpy)_2$]	0.78	0.40	−1.47	−1.75
poly[Os{Pz-$(PhIm)_2$}$(bpy)_2$]	0.75, 1.07	*a*	*b*	*b*

[a] Films were unstable in basic media. [b] Reduction of these polymers was irreversible and caused major changes in their electrochemistry.

scan in Figure 3) nor the small wave at +0.4 V in base (Figure 4). The former may be due to sites in which an adjacent noncoordinated imidazole ring has been deprotonated (structure **4**), while the later may be due to sites in which the coordinated imidazole ring has not been protonated due to pH encapsulation (structure **5**).[16]

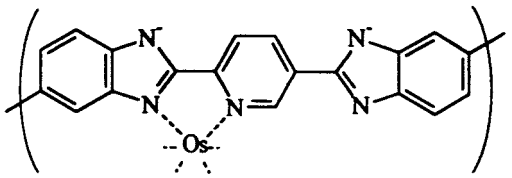

4

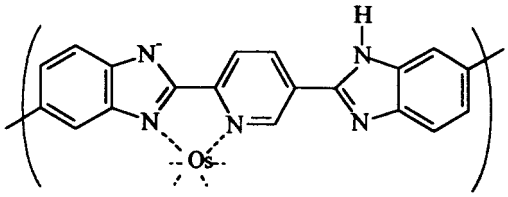

5

The cyclic voltammetry of poly[Os{Pz-$(PhIm)_2$}$(bpy)_2$] under acidic conditions has been previously described.[10] The Os(III/II) wave is split into two components by strong electronic coupling across the pyrazine ring. Formal potentials are given in Table 1. The first wave occurs at a slightly less (ca. 30 mV) positive potential than the main oxidation of poly[Os{Py-$(PhIm)_2$}$(bpy)_2$] in acid, while the second wave is significantly (290 mV) more positive. Voltammetry of poly[Os{Pz-$(PhIm)_2$}-$(bpy)_2$] at negative potentials, or under basic conditions, failed to give useful results because of the instability of the polymer.

Figure 5 shows voltammograms of two poly[Ru{Pz-$(PhIm)_2$}-$(bpy)_2$] films under acidic conditions. The solid curve is for a metallopolymer sample prepared with an excess of $Ru(bpy)_2Cl_2$, so that almost all of its pyrazine rings were complexed to two Ru centers. As for the Os analogue, this fully loaded polymer shows a splitting of the Ru(III/II) wave into two almost equal components. Their formal potentials are reported in Table 1. The smaller separation of the two waves (0.16 V) relative to poly[Os{Pz-$(PhIm)_2$}$(bpy)_2$] (0.32 V) indicates that metal−metal coupling across the pyrazine ring is significantly weaker.

The dashed curve in Figure 5 is for a metallopolymer prepared with only one equivalent of $Ru(bpy)_2Cl_2$ per pyrazine ring. The resulting lower number of pyrazine rings complexed to two Ru centers is indicated by the smaller size of the 1.29 V wave relative to the 1.13 V wave. A third wave for Ru sites complexed to nonbridging (singly coordinated) pyrazine rings is not resolved, although the broadening and slight positive shift of the 1.13 V wave and the higher currents between the two waves clearly indicate that one is present in the 1.15−1.20 V region.

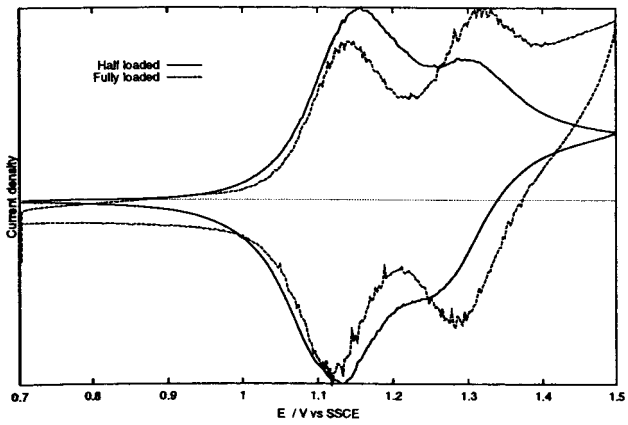

Figure 5. Cyclic voltammetry (100 mV s^{-1}) of two poly[Ru{Pz-$(PhIm)_2$}$(bpy)_2$] samples on Pt disk electrodes in 2:1 CH_2Cl_2:CH_3CN containing 0.1 M Et_4NClO_4 and two drops of 70% $HClO_4$.

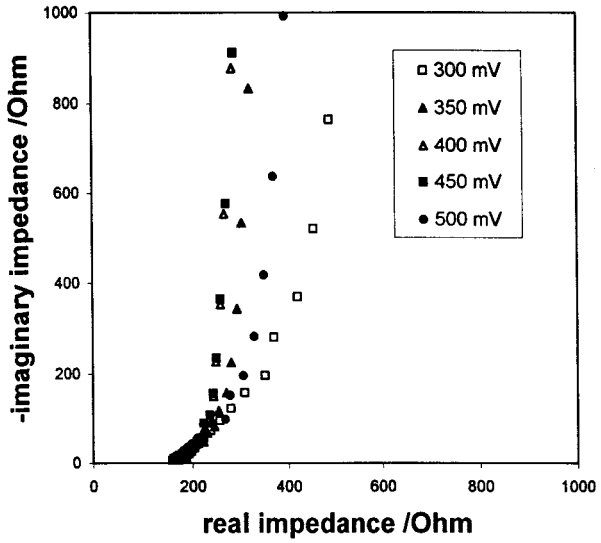

Figure 6. Complex plane impedance plots for a ca. 85 nm thick film of poly[Os{Py-$(PhIm)_2$}$(bpy)_2$] on a glassy carbon disk electrode (0.071 cm^2) at various potentials in CH_3CN containing 0.1 M Et_4NClO_4.

Impedance Spectroscopy. Figure 6 shows complex plane impedance plots at various dc potentials for a poly[Os{Py-$(PhIm)_2$}$(bpy)_2$] film in a neutral CH_3CN electrolyte. Each plot shows two distinct regions, as predicted by the finite transmission line[17] and other models of redox polymer systems.[18,19] Extrapolation of the high frequency 45° region to the real (Z') axis gives a resistance (R_{high}) equal to the uncompensatated solution resistance R_s (the lack of a significance dependence of R_{high} on potential indicates that any contribution from the film's ionic resistance is negligible). R_e, the electronic resistance of the film, is given by eq 1[17]

$$R_e = 3(R_{low} - R_{high}) \quad (1)$$

where R_{low} is the Z' intercept of the nearly vertical low-frequency region of the impedance plot. The electron diffusion coefficient D_e may then be found from[18]

$$D_e = d^2/C_{low}R_e \quad (2)$$

where d is the thickness of the film and C_{low} is its low-frequency capacitance, which can be obtained from the slope of a plot of the imaginary impedance (Z'') vs $1/\omega$ (ω is frequency in rad s^{-1}).

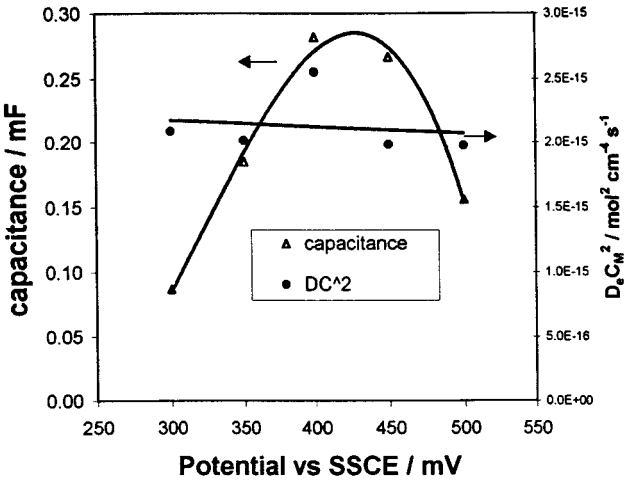

Figure 7. Low-frequency capacitances and $D_eC_M^2$ values from the impedance data shown in Figure 6.

Because it is very difficult to determine film thicknesses with acceptable accuracy,[9] we will report values of $D_eC_M^2$, where C_M is the concentration of redox active metal sites in the film. Thus, D_e/d^2 values from eq 2 are converted to $D_eC_M^2$ values by using the surface concentration of active sites Γ_M ($= C_Md$) determined from the area under a slow voltammogram. The use of $D_eC_M^2$ has literature precedent and provides for safer comparisons between different materials.

Figure 7 shows plots of C_{low} and $D_eC_M^2$ values extracted from the impedance data shown in Figure 6 as functions of potential. As expected, the C_{low} vs potential plot resembles a voltammetric peak with C_{low} peaking at the half-wave potential, and $D_eC_M^2$ is independent of potential. This provides good evidence that our analysis of the impedance data is valid and that neglection of the film's ionic resistance is justified. Table 2 summarizes $D_eC_M^2$ values for all of the polymers studied in this work.

Dual (Sandwich) Electrode Voltammetry.[20] In this technique, a thin film of polymer is cast on a platinum disk electrode and a thin gold film is then vapor deposited over the top of the polymer film and a second disk electrode. The potential at each side of the polymer film may then be controlled with a bipotentiostat. The gold film is sufficiently porous to permit the motion of solvent and ions between the polymer film and solution bulk.

A representative current−voltage response is shown in Figure 8 for poly[Ru{Pz-(PhIm)$_2$}(bpy)$_2$], together with a normal cyclic voltammogram for reference. Results for poly[Ru{Py-(PhIm)$_2$}(bpy)$_2$] and poly[Os{Pz-(PhIm)$_2$}(bpy)$_2$] have previously been published.[9] For the data in Figure 8, the gold coating was held at a potential (0.3 V) well below the first formal potential, while the potential of the polymer-coated electrode was swept through the Ru(III/II) waves. At sufficiently high potentials, oxidized Ru(III) sites begin to accumulate near the Pt electrode surface. As the potential increases, a gradient forms between the oxidized Ru(III) sites near one electrode and the reduced Ru(II) sites near the other. As these positive sites move through the film (or, conversely, as electrons move through it in the opposite direction) a current develops between the two electrodes. The limiting current, which can develop as a result of this gradient, is related to D_e as derived[20] from Fick's first law and is described by eq 3.

$$i_{lim} = nFAD_eC_M^2/\Gamma_M \quad (3)$$

Γ_M was determined by cyclic voltammetry following removal of the gold film with mercury.

The response shown in Figure 8 for poly[Ru{Pz-(PhIm)$_2$}(bpy)$_2$] is unusual in that it consists of two separate waves. However, this is perhaps not surprising because they correspond to the two voltammetric waves.[10] Although it is difficult to accurately measure the individual limiting currents for the two waves in the dual electrode voltammogram in Figure 8, they can be seen to be approximately equal. Thus D_e values must be similar for the two processes. This is contrary to the behavior of poly[Os{Pz-(PhIm)$_2$}(bpy)$_2$], for which the second (higher potential) wave is significantly smaller than the first.[10]

Table 2 summarizes $D_eC_M^2$ results for the other polymers. Poly[Ru{Py-(PhIm)$_2$}(bpy)$_2$], poly[Os{Py-(PhIm)$_2$}(bpy)$_2$], and poly[Ru(Py-Im$_2$Ph)(bpy)$_2$] all gave single dual electrode voltammetric waves and so a single $D_eC_M^2$ value is given for each. Poly[Ru{Pz-(PhIm)$_2$}(bpy)$_2$] and poly[Os{Pz-(PhIm)$_2$}(bpy)$_2$] both gave two waves, and so individual $D_eC_M^2$ values have been estimated for each wave.

Discussion

$D_eC_M^2$ results are summarized in Table 2. As can be seen from the standard deviations in the table, the reproducibility between films was not particularly good. However, the agreement between results from the two different techniques (impedance spectroscopy and dual electrode voltammetry) are good considering this variability between films. The large uncertainties reported in Table 2 presumably arise from unevenness in the coating of the electrodes.

The $D_eC_M^2$ values reported in Table 2 range from 0.2×10^{-14} to 12×10^{-14} mol^2 cm^{-4} s^{-1} and are surprisingly high for such rigid polymers (poly[Ru{Py-Im$_2$Ph}(bpy)$_2$] is particularly rigid but still exhibits a high $D_eC_M^2$). For comparison, $D_eC_M^2$ values are 0.18×10^{-14} mol^2 cm^{-4} s^{-1} for poly-[Ru(bpy)$_2$(4-vinylpyridine)$_2$]$^{3+/2+}$,[20] 1.2×10^{-14} mol^2 cm^{-4} s^{-1} for poly-[Os(bpy)$_2$(4-vinylpyridine)$_2$]$^{3+/2+}$,[20] and 0.48×10^{-14} mol^2 cm^{-4} s^{-1} for poly-[Ru(bpy)$_2$(3-{pyrrol-1-ylmethyl}pyridine)$_2$]$^{3+/2+}$.[21] Electron transport in these nonconjugated metallopolymers presumably can only occur by outer sphere electron exchange. Since the polymers studied in this work (particularly poly[Ru{Py-Im$_2$Ph}(bpy)$_2$]) should be less flexible, they would be expected to exhibit lower $D_eC_M^2$ values. However, they are significantly higher for the Ru polymers and of similar magnitude for the Os polymers. This points to the operation of an additional electron transport mechanism in the conjugated materials studied here. The absence of ligand-based electrochemistry in the anodic electrochemistry of the metalloplymers, the Nerstian potential dependence of the dual electrode voltammetric profiles on potential, and the independence of $D_eC_M^2$ values on potential (Figure 7) all point to the absence of electron transport mediation by the backbone. The high $D_eC_M^2$ values obtained for the conjugated metallopolymers must therefore be attributed to enhancement by a superexchange mechanism, as previously concluded for poly[Ru{Py-(PhIm)$_2$}(bpy)$_2$][9] and poly{[Os{Pz-(ImPh)$_2$}(bpy)$_2$](ClO$_4$)$_2$.[10]

Closer examination of the data in Table 2 provides additional evidence for the operation of superexchange mechanisms for electron transport and allows one to assign hole and electron mechanisms in some cases. First, the fact that $D_eC_M^2$ values obtained for the protonated forms are similar for the Ru and Os polymers points to the involvement of a mechanism in addition to outer sphere electron exchange, which is faster for Os(bpy)$_3^{3+/2+}$ than for Ru(bpy)$_3^{3+/2+}$.[20] This difference is manifested in the [M(bpy)$_2$(4-vinylpyridine)$_2$]$^{3+/2+}$ polymers (compare the $D_eC_M^2$ values given above), as would be expected for electron transport by outer sphere electron exchange. That it is

TABLE 2: $D_eC_M^2$ Results (10^{-14} mol^2 cm^{-4} s^{-1}) and Standard Deviations for Multiple Films from Impedance Spectroscopy (IS) and Dual Electrode Voltammetry (DEV)

	protonated		deprotonated	
complex	IS	DEV	IS	DEV
poly[Ru{Py-(PhIm)$_2$}(bpy)$_2$]	1.5 (±0.8)[a]	0.91 (±0.5)[a]	2.6 (±0.1)[b]	12 (±0.5)[b]
poly[Ru{Py-Im$_2$Ph}(bpy)$_2$]	0.99 (±0.08)[a]			
poly[Ru{Pz-(PhIm)$_2$}(bpy)$_2$]				
1st wave	0.78 (±0.23)[c]	2.2[c,d]		
2nd wave	2.1 (±2.2)[c]	2.2[c,d]		
poly[Os{Py-(PhIm)$_2$}(bpy)$_2$]	0.71 (±0.41)[a]	0.55[a,d]	0.21 (±0.08)[e]	
poly[Os{Pz-(PhIm)$_2$}(bpy)$_2$]				
1st wave	2.0 (±1.2)[c]	3.0 (±1.4)[c]		
2nd wave	1.4 (±1.1)[c]	1.6 (±0.7)[c]		

[a] CH_3CN + 0.1 M Et_4NClO_4 + ca. 50 mM $HClO_4$. [b] CH_3CN + 0.1 M Et_4NClO_4 + ca. 5 mM Bu_4NOH. [c] 2:1 CH_2Cl_2:CH_3CN + 0.1 M Et_4NClO_4 + ca. 50 mM $HClO_4$. [d] Measurement on a single film. [e] CH_3CN + 0.1 M Et_4NClO_4 (addition of Bu_4NOH did not influence $D_eC_M^2$).

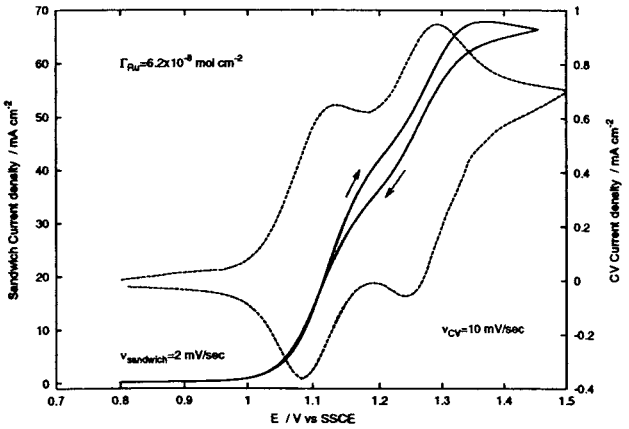

Figure 8. Dual electrode voltammetry (2 mV s^{-1}, solid line) and cyclic voltammetry (10 mV s^{-1}, dashed line) for a poly[Ru{Pz-(PhIm)$_2$}(bpy)$_2$] film ($\Gamma_{Ru} = 6.2 \times 10^{-8}$ mol cm^{-2}) on a Pt disk electrode in 2:1 CH_2Cl_2:CH_3CN containing 0.1 M Et_4NClO_4 and $HClO_4$.

not observed for the conjugated polymers studied here clearly indicates that the outer sphere mechanism is less significant.

The effects of deprotonation of the imidazole of the backbone provide even more convincing evidence for a mechanism in addition to outer sphere electron transfer and point strongly to superexchange mechanisms that differ for the Ru and Os polymers. Deprotonation of poly[Ru{Py-(PhIm)$_2$}(bpy)$_2$] causes a significant increase in $D_eC_M^2$ (by a factor of 2 or more), while deprotonation of poly[Os{Py-(PhIm)$_2$}(bpy)$_2$] has the opposite effect, decreasing $D_eC_M^2$ by a factor of ca. 3. It is difficult to envisage that deprotonation could influence outer sphere electron transport so differently for the two polymers. However, this observation can readily be explained if electron transport involves hole-type superexchange for the Ru polymer and electron-type superexchange for the Os polymer. Deprotonation has been shown to increase the strength of hole-type superexchange coupling in both the Ru and Os dinuclear analogues of these metallopolymers.[22] The increase in $D_eC_M^2$ upon deprotonation of poly[Ru{Py-(PhIm)$_2$}(bpy)$_2$] is consistent with the behavior of its binuclear analogue and consistent with a hole-type superexchange mechanism.[22] The decrease in $D_eC_M^2$ upon deprotonation of poly[Os{Py-(PhIm)$_2$}(bpy)$_2$], on the other hand, is inconsistent with hole-type superexchange but consistent with electron-type superexchange, which should be enhanced by deprotonation of the ligand. We have previously invoked electron-type superexchange to explain the lower $D_eC_M^2$ observed for the second wave of poly[Os{Pz-(PhIm)$_2$}(bpy)$_2$].[10] It was suggested that D_e is higher for the lower potential process because the Os d-orbital energy is closer to that of the polymer LUMO level.

Although the differences between $D_eC_M^2$ values for the polymers studied here and the previously studied nonconjugated polymers are quite small, the trends observed on changing the metal and the pH, and the lack of influence of backbone rigidity, all point to operation of superexchange mechanisms. In addition, it has been observed that $D_eC_M^2$ values for the conjugated polymers slowly decrease when the conjugation of the polymer is disrupted by holding in its oxidized state.[9] This indicates that $D_eC_M^2$ values for outer sphere electron transport alone in the polymers studied here are much lower than the measured $D_eC_M^2$ values reported in Table 2.

Conclusions

The $D_eC_M^2$ results reported here provide strong evidence that electron transport in Ru and Os conjugated polybenzimidazole polymers is substantially enhanced by superexchange mechanisms. There is growing evidence that an electron-type superexchange mechanism is dominant in the Os polymers, while a hole-type mechanism dominates for the Ru polymers. This implies that the M(III/II) levels of the complexes lie approximately in the middle of the HOMO−LUMO gap of the polymer backbone. It is therefore envisaged that further enhancements in electron transport rates could be obtained by raising the backbone HOMO energy for the Ru polymers, or by lowering the backbone LUMO energy for the Os polymers. The former strategy has been attempted by employing a bithiazole-bithiophene copolymer.[23] Although voltammetry of such Ru and Os metallopolymers does not show evidence of significant metal−metal coupling, preliminary results indicate that the Ru polymers exhibit $D_eC_M^2$ values that are even higher than those reported here.

Acknowledgment. This work was supported by the Natural Sciences and Engineering Research Council of Canada and Memorial University.

References and Notes

(1) Kingsborough, R. P.; Swager, T. M. *Progr. Inorg. Chem.* **1999**, *48*, 123.
(2) Pickup, P. G. *J. Materials Chem.* **1999**, *8*, 1641.
(3) Yamamoto, T.; Maruyama, T.; Zhou, Z.-H.; Ito, T.; Fukuda, T.; Yoneda, Y.; Begum, F.; Ikeda, T.; Sasaki, S.; Takezoe, H.; Fukuda, A.; Kubota, K. *J. Am. Chem. Soc.* **1994**, *116*, 4832.
(4) Wolf, M. O.; Wrighton, M. S. *Chem. Mater.* **1994**, *6*, 1526.
(5) Zhu, S. S.; Carroll, P. J.; Swager, T. M. *J. Am. Chem. Soc.* **1996**, *118*, 8713.
(6) Zhu, S. S.; Swager, T. M. *J. Am. Chem. Soc.* **1997**, *119*, 12568.
(7) Buey, J.; Swager, T. M. *Angew. Chem., Int. Ed. Engl.* **2000**, *39*, 608.
(8) Cameron, C. G.; Pickup, P. G. *Chem. Commun.* **1997**, 303.
(9) Cameron, C. G.; Pickup, P. G. *J. Am. Chem. Soc.* **1999**, *121*, 11773.
(10) Cameron, C. G.; Pickup, P. G. *J. Am. Chem. Soc.* **1999**, *121*, 7710.

(11) Creutz, C. *Progr. Inorg. Chem.* **1981**, *30*, 1.
(12) Haga, M.; Ale, M. M.; Koseki, S.; Yoshimura, A.; Nozaki, K.; Ohno, T. *Inorg. Chim. Acta* **1994**, *226*, 17.
(13) Lay, P. A.; Sargeson, A. M.; Taube, H. *Inorg. Synth.* **1986**, *24*, 291.
(14) Sawyer, D. T.; Roberts, J. L. *Experimental Electrochemistry for Chemists*; Wiley: New York, 1974.
(15) Osaheni, J. A.; Jenekhe, S. A. *Macromolecules* **1995**, *28*, 1172.
(16) Sameuls, G. J.; Meyer, T. J. *J. Am. Chem. Soc.* **1981**, *103*, 307.
(17) Albery, W. J.; Elliott, C. M.; Mount, A. R. *J. Electroanal. Chem.* **1990**, *288*, 15.
(18) Mathias, M. F.; Haas, O. *J. Phys. Chem.* **1992**, *96*, 3174.
(19) Vorotyntsev, M. A.; Badiali, J. P.; Vieil, E. *Electrochim. Acta* **1996**, *41*, 1375.
(20) Pickup, P. G.; Kutner, W.; Leidner, C. R.; Murray, R. W. *J. Am. Chem. Soc.* **1984**, *106*, 1991.
(21) Ochmanska, J.; Pickup, P. G. *J. Electroanal. Chem.* **1991**, *297*, 197.
(22) Haga, M.; Ano, T.; Kano, K.; Yamabe, S. *Inorg. Chem.* **1991**, *30*, 3843.
(23) MacLean, B. J.; Pickup, P. G. *J. Materials Chem.* **2001**, *11*, 1357.